Evaluation of Solution-Processed Reduced Graphene Oxide Films as Transparent Conductors

Héctor A. Becerril,[†] Jie Mao,[‡] Zunfeng Liu,[‡] Randall M. Stoltenberg,[†] Zhenan Bao,[†,*] and Yongsheng Chen[‡,*]

[†]Department of Chemical Engineering, Stanford University, 381 North-South Mall, Stanford, California 94305, and [‡]Key Laboratory for Functional Polymer Materials and Center for Nanoscale Science & Technology, Institute of Polymer Chemistry, College of Chemistry, Nankai University, Wenjin Rd 94, Tianjin 300071, China

ABSTRACT Processable, single-layered graphene oxide (GO) is an intriguing nanomaterial with tremendous potential for electronic applications. We spin-coated GO thin-films on quartz and characterized their sheet resistance and optical transparency using different reduction treatments. A thermal graphitization procedure was most effective, producing films with sheet resistances as low as $10^2 - 10^3$ Ω/square with 80% transmittance for 550 nm light. Our experiments demonstrate solution-processed GO films have potential as transparent electrodes.

KEYWORDS: transparent conductors · graphene · solution processed · displays · solar cells

Graphene oxide (GO) is a water-soluble nanomaterial prepared through extensive chemical attack of graphite crystals to introduce oxygen containing defects in the graphite stack,[1] followed by complete exfoliation of the solid into sheets of atomic thickness by either thermal or mechanical treatments.[2–4] According to a recently proposed model, GO sheets are composed of planar, graphene-like aromatic domains of random sizes interconnected by a network of cyclohexane-like units in chair configuration which are decorated by hydroxy, epoxy, ether, diol, and ketone groups.[5] These functional groups in GO impart water solubility to the individual sheets, and removal of such groups results in flocculation and precipitation.[6] Solution-processable GO has been used to fabricate paper-like films with excellent mechanical properties,[7] as well as electrically conductive polymeric[8,9] and ceramic composites.[10] Importantly, the electrical conductivity of GO and its composite formulations is typically enhanced through removal of the oxidized moieties in the sheets by chemical reduction, which takes place after the material has been processed into the final form.[3] The reduced GO inevitably contains lattice defects[2] that degrade its electrical properties compared to pristine graphene sheets obtained by the tape-peeling method,[11] but the solution-processing compatibility of GO make the material attractive for large area applications. So far, few layer, chemically reduced GO films with sheet resistance of ~4 MΩ/square,[12] and nanocomposite silica/GO films with conductivities as high as ~0.5 S/cm (sheet resistance R_s ~800 kΩ/square for a 25 nm film) have been reported.[10] Such level of conductivity is however not sufficient for transparent electrode applications where intensive charge injection or large area format is required, such as liquid crystal displays.[13,14] Here we explore the direct use of GO for fabricating solution-processed, all-GO thin-films with high electrical conductivity and varying degrees of transparency. We compare the efficiency of chemical and thermal reduction methods for treating our films and report that a high-temperature graphitization treatment is most effective in deoxygenating the films and restoring conductivity. Similar thermal processes have been successfully used to remove oxygen-containing functional groups from carbon nanotubes[15] and to fabricate transparent electrodes from thin photoresist films.[16] We obtain films with conductivities in the order of 10^2 S/cm (R_s < 1 kΩ/square) with greater than 80% light transmittance in the 400–1800 nm wavelength range. The significantly enhanced conductivity of our films arises from a more complete reduction than that achieved with chemical methods, and this finding suggests that through further process development GO films could become attractive for large-area transparent electrode applications.

*Address correspondence to zbao@stanford.edu, yschen99@nankai.edu.cn.

Received for review November 19, 2007 and accepted January 29, 2008.

Published online February 9, 2008.
10.1021/nn700375n CCC: $40.75

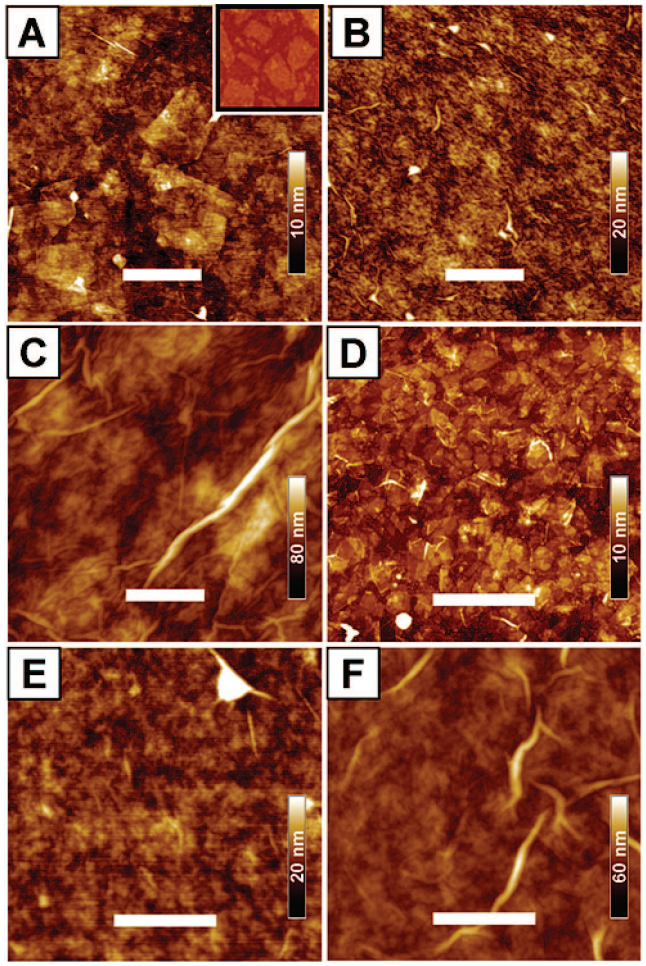

Figure 1. Tapping mode AFM height images of spin-coated GO films. (A) 3 nm thick, continuous GO film clearly showing edges of individual GO sheets. Surface rms roughness (R_q) is 1.2 nm. Inset: Detail of a submonolayer film depicting isolated sheets in a 1 × 1 μm field. (B) 8 nm film showing GO sheets deposited in a disordered manner. R_q is 2.2 nm. (C) 20 nm film showing the rough, wrinkled morphology seen in thicker (>15 nm) GO spin-coated films. R_q is 8.1 nm. (D) Hydrazine vapor treated (18 h) 3 nm GO film. R_q is 1.3 nm. (E) A 30 nm GO film treated by a combination of hydrazine vapor for 18 h and thermal annealing at 400 °C for 3 h. R_q is 2.4 nm. (F) Image of a 67 nm film after vacuum annealing at 1100 °C. R_q is 4 nm. White bar is 1 μm in all images, and the thicknesses reported for (D−F) were measured after reduction.

RESULTS AND DISCUSSION

Preparation of GO Solutions and Films. We synthesized our water-processable single-layer GO by a modified Hummers method.[17] Briefly, a small amount of flake graphite (Qingdao Tianhe Graphite Co. Ltd., Qingdao, China) was vigorously stirred for 5 days in a solution of $NaNO_3$ and $KMnO_4$ in concentrated H_2SO_4, washed with 5 wt % H_2SO_4 in water and reacted with a 30 wt % aqueous solution of H_2O_2 to complete the oxidation. Inorganic anions and other impurities were removed through 15 washing cycles that included centrifugation, discarding supernatant liquid, and resuspending the solid in an aqueous mixture of 3 wt % H_2SO_4 and 0.5 wt % H_2O_2 using stirring and ultrasonication. Another set of centrifugation and washing procedures was effected three times using 3 wt % HCl in water as the dispersion medium and then one more time using purified water to resuspend the solids. This suspension was passed through a weak basic ion-exchange resin (Styrene-DVB D301T, Tianjin Nankai Hecheng S&T Co, Ltd.) to remove remaining acid. Finally the material was dried to obtain a loose brown powder which can be stored indefinitely.

For thin-film fabrication from GO, the powder was first suspended in water by ultrasonication and centrifugated at 14000 rpm to remove multilayer species, which constituted ~10% of the powder by weight. The carefully recovered supernatant is a solution of single-layer GO with concentration as high as ~15 mg/mL and is stable against precipitation for several months. We used single-layer GO solutions to deposit the GO films on piranha-cleaned (caution: piranha mixture is a strong oxidizer), (aminopropyl)triethoxysilane (APTES) treated, glass and quartz surfaces. Testing film deposition by spin-coating, drop-casting, and solvent-induced precipitation revealed that spin-coating produces more uniform although thinner films than the other methods, and this technique was used for all films presented here. Typically, the substrate was completely covered with sufficient amount of the GO solution, allowed to stand for 60 s and spin coated at 500, 800, and 1600 rpm for 30 s each. After spin coating the GO films were dried at 100 °C in a vacuum oven and stored in ambient conditions in sealed plastic containers.

Morphology of GO Films before and after Reductive Treatments. We used an atomic force microscope (AFM, Multimode Nanoscope IIIa with Extender electronics, Veeco Metrology Inc., Santa Barbara, CA) and a profilometer (Dektak 150, Veeco Metrology Inc.) to probe film morphology and thickness (see Supporting Information). Figure 1, panels A−C, display characteristic AFM images of as-deposited GO films of different thicknesses. We observed that the film morphology changes significantly with this dimension. Panel A shows a typical film spin coated from a low concentration GO solution (<2 mg/mL). Such films are ~3 nm thick, continuous and it is possible to distinguish the edges of individual sheets. The inset in (A) depicts a submonolayer GO film on a quartz substrate showing separated GO sheets. From analysis of multiple similar images, we find that the average lateral dimension of individual GO sheets is ~364 nm with a relative standard deviation (rsd) of 33% while the average sheet height, including kinked and wrinkled areas, is 1.4 nm with a 12% rsd, comparable to the 1.1 nm with 18% rsd observed by other groups for GO on mica.[3,6,18] Such sheet thickness value has been suggested to indicate presence of oxidized functional groups on both sides of single GO sheets, and the slight discrepancy in height is likely related to the different substrate. Figure 1B is representative of the topology of films spin coated from GO solutions with concentrations in the 4−8 mg/mL range. We obtain films between 6 and 15 nm in thickness, and

we observe increased disorder and roughness and the appearance of micrometer-long wrinkles, and it becomes increasingly hard to identify edges of the separate sheets. Finally, films deposited from high concentration solutions (12–15 mg/mL) are thicker (~20 nm) and rougher, individual flakes are not resolvable, and there are extensive networks of long, broad wrinkles across the film surface (Figure 1C). Films up to ~ 150 nm can be deposited through repeated spin-coating from these high-concentration solutions. In general we observe that film thickness increases continuously and not in multiples of individual sheet height, again indicating that the films have a significant degree of disorder, likely resulting from the fast dynamics of deposition by spin coating and from the flexible nature of the GO sheets.[5]

Next we evaluated the effect of different chemical and thermal reduction treatments on the morphology of GO films. We used hydrazine monohydrate in our chemical reduction procedures since it has been reported to achieve the highest degree of reduction of GO in solution.[3] Unfortunately, immersing our GO films in hot aqueous hydrazine solutions (80 °C) resulted in film fragmentation and delamination even on substrates that had been treated with APTES adhesion layers, so we utilized an alternative hydrazine vapor reduction scheme described in the methods section. For thermal treatments, we experimented with heating our films under nitrogen flow, argon flow, or vacuum, at temperatures ranging from 400 to 1100 °C. Importantly, while it is known that graphene oxide is thermally unstable,[18] rapid heating of such material to ~1050 °C can be used to exfoliate GO sheets through the large pressures generated during gasification of oxygenated functional groups intercalated between graphite oxide layers.[2,4] Additionally, high-temperature treatments (>1000 °C) have also been used to prepare graphene films from SiC substrates,[20,21] We therefore hypothesized that controlled high-temperature treatments could gradually pyrolyze and remove oxygenated functional groups from the GO sheets, reducing them into the more temperature-stable graphene. Indeed, the results we present here show that high-temperature thermal treatments can, under certain conditions, produce highly reduced GO films. Very recently, during review of this paper, another research group has reported effective reduction of graphene oxide using a similar high-temperature graphitization method at 1100 °C.[22]

Panels D−F of Figure 1 are micrographs of films that underwent different reduction treatments. In general, we observe that the reduction does not drastically alter the appearance of the films. The image in Figure 1D is from a ~3 nm film that was chemically reduced by exposure to an atmosphere of hydrazine monohydrate vapor at 40 °C for 18 h and dried in a vacuum oven at 80 °C for 3 h. Individual, well-defined sheets are still present, and the overall roughness is still comparable to that of the untreated film in Figure 1A of similar thickness. Figure 1E shows a typical film exposed to a combination of chemical and thermal treatments. This ~30 nm thick sample was treated with hydrazine monohydrate vapor at 40 °C for 18 h and dried similarly to the film in Figure 1D, and then the film was heated to 400 °C in a flow of ultrapure argon for 3 h inside of an in-house-built tube oven. The appearance of the sample shares features from Figure 1, panels B and C. Figure 1F shows an image of a ~60 nm film which received only a high-temperature graphitization treatment. The sample was spin coated, dried in a vacuum oven at 80 °C for 3 h, and heated to 1100 °C for 3 h at a pressure of $<10^{-5}$ Torr in a quartz tube furnace fitted with a turbomolecular pump. The AFM shows that the substrate contains abundant GO material, and the film displays the typical morphology of a thick GO sample (Figure 1C). Importantly, when working at 1100 °C a quality vacuum is critical for the successful recovery of GO material, otherwise the films can be quickly lost, likely through reaction with residual oxygen in the system. Complete loss of GO was not observed in 3 h runs at temperatures of 400, 600, and 800 °C in vacuum, and we also successfully recovered GO samples after treating them for as long as 7 h at 400 °C under Ar flow. These findings illustrate that GO materials can be heat-processed with significant degree of freedom. Figure 2 shows a thermogravimetric analysis (TGA) trace and a differential scanning calorimetry (DSC) curve of our untreated GO powder which mainly show ~30% mass loss with onset around 200 °C due to desorption of CO, CO_2, and other oxygenated carbon species as has been observed in other studies.[3,4,19]

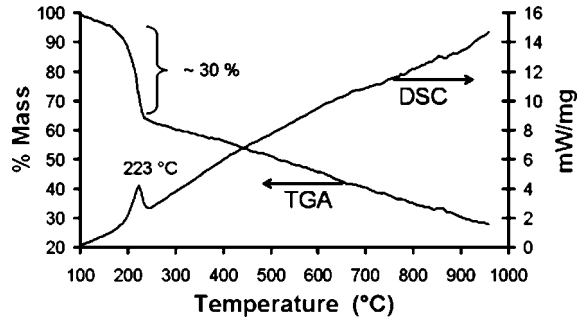

Figure 2. Thermal analysis of GO powder. TGA shows ~30% mass loss with onset ~200 °C and a relatively monotonous profile after. The DSC trace shows a correlated desorption peak centered ~223 °C. About 30% of the film was retained at temperatures as high as 1000 °C for this particular run.

Characterization of Reduced GO Films. After the reduction treatments, we patterned 40 nm gold contacts onto GO films through a shadow mask and determined their sheet resistance using a semiconductor parametric analyzer (Keithley 4200, Keithley Instrumetns Inc., Cleveland, OH). We also probed the optical transmittance of the films at 550 nm wavelength, using a UV–vis−NIR spectrophotometer (Carey 6000i, Varian Inc.), and mea-

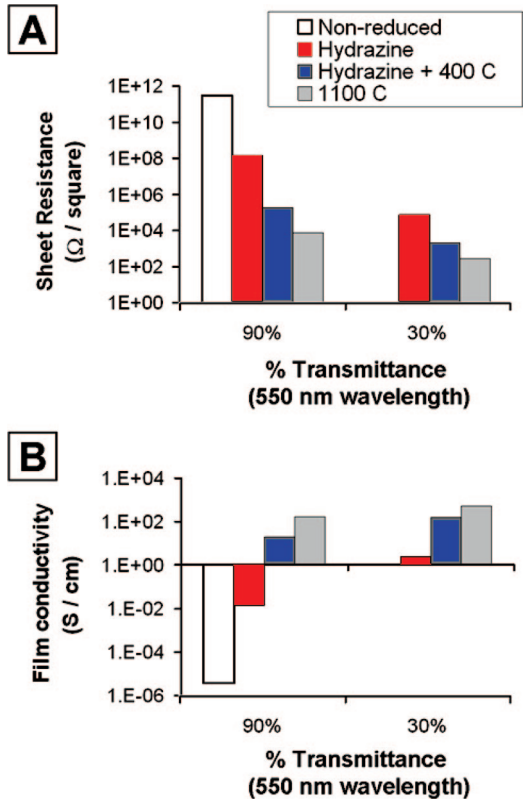

Figure 3. Comparison of the electrical properties of GO films of different optical transparency after undergoing different reduction treatments. (A) Measured sheet resistance of the films. (B) Film conductivity calculated from the sheet resistance and the film thickness. Thickness of the films in the 90% transmittance group is 8.5, 5.0, 2.9, and 8.1 nm from left to right. The corresponding thickness averages are 55.3, 30.9, and 66.9 nm for the films in the 30% transmittance group.

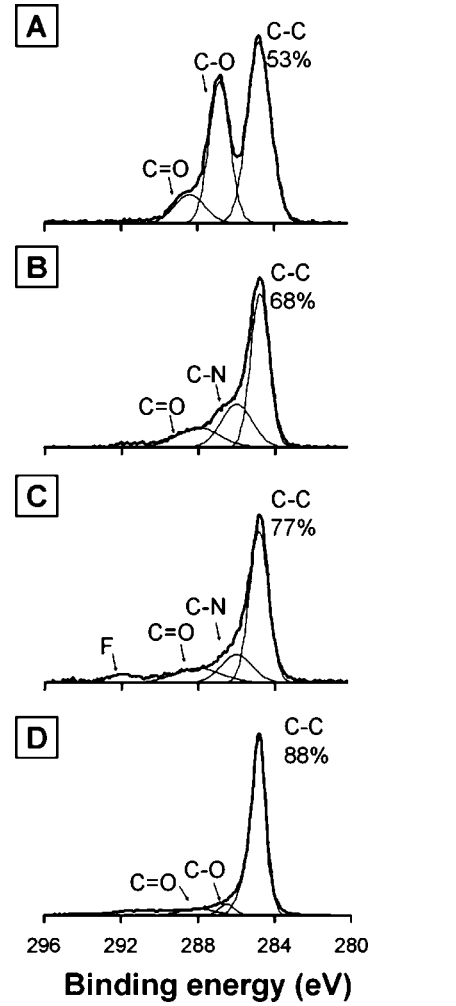

Figure 4. High-resolution XPS analysis of the effect of different reduction treatments on the GO films. Deconvolution revealed the presence of C—C (~284.8 eV), C—N (~285.7 eV), C—O (286.2), C═O (~287.8 eV) species in the film. The percentage of deoxidized carbon (C—C, ~284.5 eV) in each film is indicated in the figure. (A) Nonreduced film. (B) Hydrazine-vapor treated film. (C) Hydrazine-vapor plus annealing at 400 °C. (D) Thermal annealing at 1100 °C in vacuum. The significant C—N signal in panels C and D suggests formation of hydrazone groups during the hydrazine treatment. The F signal at ~292 eV, most evident in panel C, is caused by contamination from the vacuum system.

sured film thickness using AFM or profilometry. Figure 3A presents two groups of films with distinct optical transmittance, which include a nonreduced film and films treated with hydrazine vapor, hydrazine-vapor plus 400 °C annealing, and 1100 °C graphitization, and compares their respective sheet resistance. In general, thinner (thicker) films are more (less) transparent irrespective of reduction method, but within each group the thickness of individual films can vary. In Figure 3B the thickness of the films has been used to calculate the conductivity of the samples in panel A. Both figures clearly show a trend in the electrical properties of films reduced by different methods, with sheet resistance (conductivity) decreasing (increasing) in the order unreduced < hydrazine vapor < hydrazine plus 400 °C annealing < 1100 °C graphitization. To elucidate the causes behind this trend, we used X-ray photoelectron spectroscopy (XPS, PHI-5000 Versaprobe, ULVAC-PHI Inc., Osaka, Japan) to probe effect of the different reduction treatments on the composition of the GO films.

Figure 4 shows high-resolution narrow scans from the carbon region of nonreduced and reduced films, with the three most prominent deconvoluted components of the C 1s envelope shown in each panel. This analysis revealed that the relative content of carbon not bound to oxygen (C−C, ~284.5 eV peak) follows the same trend as the film conductivity. We also observed substantial incorporation of nitrogen in both hydrazine-treated samples (Figure 4, panels B and C), and the presence of this element in these films was confirmed by XPS analysis of the nitrogen region (see Figure 5, panels B and C). Similar nitrogenated carbon signals in hydrazine-treated GO have been observed and attributed to partial reduction of carbonyl functionalities to hydrazone groups.[3,6] We see that annealing at 400 °C reduces the nitrogenated carbon content, likely through desorption of nitrogen. These results indicate that chemical reduction with hydrazine vapor alone is less efficient than the other two methods of GO reduc-

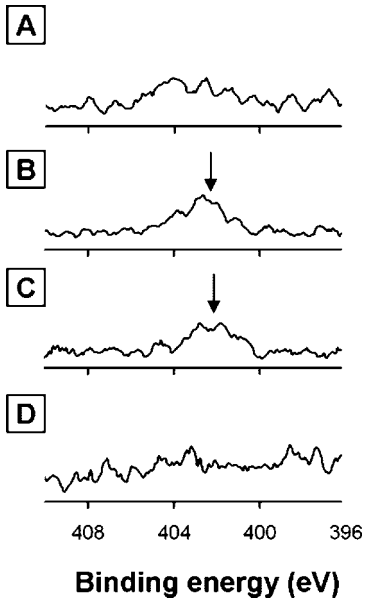

Figure 5. High-resolution XPS narrow scans of the N 1s region for the films in Figure 4. (A) Nonreduced GO film material deposited on an APTES-treated quartz slide shows slight indication of nitrogen, possibly from the APTES layer. (B) Hydrazyne-vapor treated sample shows a well-defined and significant nitrogen peak (arrow). (C) Sample treated with hydrazine vapor plus annealing at 400 °C under argon flow clearly shows nitrogen content, although in less degree than (B), likely because of the thermal treatment. (D) Film graphitized at 1100 °C shows no nitrogen signal.

tion because it generates a substantial amount of partially reduced byproducts. Stankovitch *et al*. have obtained similar conclusions from their analysis of GO reduced in hydrazine solutions.[3] Since our goal is to find out the best possible performance of GO transparent electrodes, we did not pursue it further in this work. However, investigation of an efficient chemical reduction method is essential for reduction of annealing temperature in the future. Our XPS results also show that the conductivity enhancement that we observe between films treated with hydrazine and those treated with the combination of hydrazine and 400 °C annealing is due to a real chemical difference and is not due to improved sheet to sheet contact caused by film consolidation during the annealing step, as was proposed in the case of GO−silica composites.[10] Finally, when considered together with the electrical characterization data, the XPS analysis shows that even a relatively modest increase in the content of nonoxygenated carbon causes a significant boost in electrical performance.

Next we prepared spin-coated GO films of various thicknesses and reduced them through the combined hydrazine−400 °C treatment or the 1100 °C graphitization method. Figure 6A is a photograph of a series of GO films deposited on quartz slides, where the leftmost sample is an unreduced GO control and the rest are high-temperature-reduced GO films with thickness increasing from left to right. There is a marked transmission difference between the nonreduced and the reduced material that is evident when comparing the first and third films from the left, which have similar thicknesses. This darkening of the reduced material has been observed previously[8] and suggests partial restoration of the π-electron system in the GO. We find that, independent of thickness, our films have a flat optical transmittance profile across the visible and near-infrared region of the spectrum (Figure 6B), making them potentially desirable for solar cell,[23] display, and optical communication applications.[24] Indeed, by plotting sheet resistance *versus* optical transmittance at 550 nm wavelength of our films (see Figure 6C), we iden-

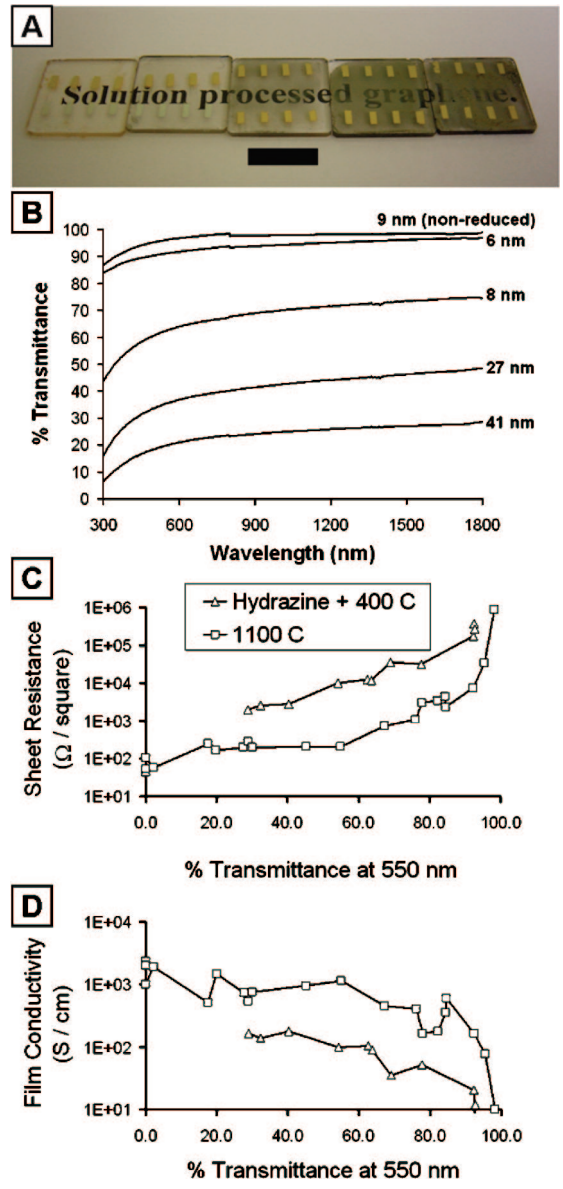

Figure 6. Optical and electrical characterization of spin-coated GO films on quartz. (A) Photograph of an unreduced (leftmost) and a series of high-temperature reduced GO films of increasing thickness. Black scale bar is 1 cm. (B) Optical transmittance spectra of the films in (A) with the film thickness indicated. (C) Comparison of the dependence of sheet resistance *vs* optical transmittance to 550 nm light for films reduced using two different methods. (D) Film conductivity *vs* % transmittance for films shown in (C).

tify graphitized films that already have sheet resistances in the $10^2 - 10^3$ Ω/square range with 80% light transmittance. Such values are significantly higher than those obtained with previously reported graphene-based materials[10] and are comparable to those obtained with carbon nanotube network transparent electrodes used for solar cells[23,25] and other applications.[26,27] In fact, some of the graphitized films in Figure 6D show conductivities of $\sim 10^3$ S/cm, less than 2 orders of magnitude lower than that for indium tin oxide (ITO).[10,28] Importantly, during review of our manuscript Wang *et al.* published a similar high-temperature graphitization procedure for reduction of GO films and obtained a conductivity of 550 S/cm[2] with a transparency of ~70% at 1000 nm,[22] which is also consistent with our results.

We note that despite the high performance of the films that we prepared, the temperature used for graphitization needs to be significantly reduced for this process to be useful in practice, so that it becomes compatible with glass or plastic substrates. Nevertheless, this study shows the potential of GO for transparent electrodes. We expect that through enhanced chemical manipulation of the solution-processable GO the oxygenated groups can be transformed into less resilient functionalities which can be more completely removed after film processing using mild conditions. Different research groups have already reported the derivatization of GO with isocyanates[29] and octadecylamine[30] mainly with the goal of providing enhanced solubility of GO in polar organic solvents. Another group has recently reported reduction of graphite fluoride with alkyl lithium reagents as an alternative route to solution processable graphene.[31] We propose that such transformations of the chemical groups in graphene oxide can play an important role in facilitating complete reduction and achieving higher film conductivities per unit thickness, possibly allowing the use of thinner films to also improve transparency. The importance of realizing these studies lies in the abundance, high-purity, and relatively inexpensive nature of graphite and GO when compared to carbon nanotubes and ITO, as well as the fact that devices fabricated with GO films would not experience ion-diffusion degradation known for ITO-based devices.[32] Developing more efficient and practical GO reduction schemes will be the object of future research, while preliminary evaluation of our GO electrodes in device applications is currently underway.

CONCLUSIONS

We reported water-processable GO thin films and investigated the relative efficiencies of chemical and thermal reductive treatments in enhancing the electrical performance of the films. We evaluated the potential of our highly reduced GO thin films as transparent conductors and identified graphitization conditions that produce films with sheet resistance and transparency levels comparable to carbon nanotube networks, but substantial improvements in the reduction method must be made before it can have serious practical applications. We have proposed a possible route for addressing this issue and identified the significant advantages that such optimized material would have as an inexpensive, abundant, transparent conductor.

METHODS

Preparation of Water-Soluble, Single-Layered Graphene Oxide. Graphene oxide was prepared using modified Hummers method[16] from flake graphite (average particle diameter of 4 μm, 99.95% purity, Qingdao Tianhe Graphite Co. Ltd., Qingdao, China). Briefly, 5 g of graphite and 3.75 g of $NaNO_3$ (A.R.) were placed in a flask. Then, 375 mL of H_2SO_4 (A.R.) was added with stirring in an ice-water bath, and 22.5 g of $KMnO_4$ (A.R.) were slowly added over about 1 h. Stirring was continued for 2 h in the ice-water bath. After the mixture was stirred vigorously for 5 days at room temperature, 700 mL of 5 wt % H_2SO_4 aqueous solution was added over about 1 h with stirring, and the temperature was kept at 98 °C. The resultant mixture was further stirred for 2 h at 98 °C. The temperature was reduced to 60 °C, 15 mL of H_2O_2 (30 wt % aqueous solution) was added, and the mixture was stirred for 2 h at room temperature.

To remove the ions of oxidant and other inorganic impurity, the resultant mixture was purified by repeating the following procedure cycle 15 times: centrifugation, removal of the supernatant liquid, addition of 2 L of a mixed aqueous solution of 3 wt % H_2SO_4/0.5 wt % H_2O_2 to the bottom solid, and dispersing the solid using vigorous stirring and bath ultrasonication for 30 min at a power of 140 W. Then a similar procedure was repeated: three times using 3 wt % HCl aqueous solution (2 L) and one time using H_2O (2 L). The final resultant water solution was passed through a weak basic ion-exchange resin (D301T, Nankai University Chemical Plant) with water as mobile phase to remove the remaining HCl acid. Then water was removed through a drying process for the collected water solution to yield 3.5 g of product.

Substrate Preparation and Deposition of GO. Glass slides, 8 × 25 mm, or 3 mm thick 1.5 × 1.5 cm quartz squares were cleaned in piranha solution (7:3 H_2SO_4:H_2O_2 mixture, **caution** extremely corrosive and highly exothermic) for 40 min followed by extensive rinsing with deionized water, dried under a nitrogen stream, and stored in a vacuum oven at 80 °C until use, typically within a period of 2 h. Substrates were treated in a dry glovebox with a 3% solution of (aminopropyl)triethoxysilane in anhydrous toluene for 1 h at room temperature, rinsed with and sonicated in anhydrous toluene, and dried under a nitrogen stream to form an APTES adhesion layer with a contact angle ~67°. Aqueous solutions of GO were deposited on the prepared substrates and allowed to wet the surface for 1 min, after which the slide was allowed to spin at 600 rpm for 1 min to cause uniforml spreading of the solution on the substrate, then at 800 rpm for 1 min to thin the solution layer, and finally at 1600 rpm for 1 min to dry the film. Films were further dried by placing them in a vacuum oven at 80 °C for 3 h before any reducing treatments.

Hydrazine Vapor Reduction. GO films on quartz slides were placed in a perfectly cleaned glass Petri dish inside a larger glass Petri dish which also contained 1 mL of hydrazine monohydrate 98% (Alfa Aesar, Ward Hill, MA). The larger dish was covered with a glass lid, sealed with Parafilm tape, and placed over a hot plate at 40 °C for 18 h, after which the dish was opened and the films were rinsed with purified water and dried both under a nitrogen stream and by heating to 80 °C in vacuum. GO films changed

color after the hydrazine vapor treatment, from matte brown to metallic gray, indicating reduction of the material. Additionally we experimented with treating our GO samples with hydrazine vapor at room temperature and at 80 °C. In all cases we observed the same color change in the films, but partial film delamination occurred in some of the samples treated at 80 °C. We selected 40 °C as the working temperature for all subsequent treatments since it provided a standard condition across sample batches and did not damage the films.

400 °C Thermal Annealing under Argon Flow. Dry GO films on quartz slides were loaded inside a 2 cm internal diameter cylindrical quartz boat with open ends. The boat was introduced in a 1 in. internal diameter glass tube oven fitted with controlled vacuum and gas flows. Films were heated under a continuous flow of 70 standard cubic centimeters of ultrapure argon, at a rate of 20 °C/min, and held a the 400 °C for 3 h, and allowed to cool to room temperature over ~1 h.

1100 °C Graphitization in Vacuum. Dry GO films on quartz were placed in quartz boats inside a 3 ft long 1 in. diameter quartz tube with one end closed. The tube was introduced into a Lindberg/BlueM split hinge oven (Lindberg/Blue M 3-zone tube oven, Blue-M, White Deer, PA) and the open end was fitted to a turbopump vacuum line (Turbo-V 250 MacroTorr, Varian Inc., Palo Alto, CA). Films were heated to 100 °C at ambient pressure, then the turbo pump was switched on and a vacuum of $\sim 10^{-5}$ Torr was established before heating to 1100 °C. Heating rates as high as 20 °C/min could be achieved without loss of films. The temperature was held constant at 1100 °C for 3 h after which the system was allowed to cool down (~3 h). At room temperature ambient air was admitted to the tube and the films were recovered and stored as mentioned above. Heating rate and treatment duration were determined empirically. We found that the initial heating from room temperature to ~300 °C must be done slowly (<10 °C) to avoid complete film loss by rapid evolution of CO, CO_2, and water vapor. Some gradual film loss also occurs during heating from 300 to 1100 °C as can be appreciated in the TGA trace in Figure 2. This can be minimized by keeping the heating rate below 20 °C/min, but batch to batch variation of the GO material prevents us from drawing more specific conclusions. Similarly, the length of the graphitization step at 1100 °C treatment was varied between 2 and 7 h and we found that 3 h was the longest time with acceptable sample yield (>40%). Importantly, the choice of 1100 °C as the graphitization temperature was guided by related literature reports.[2,4,15,20,21] Finally, we expect that performing the graphitization treatment under a flow of inert gas would eliminate the problem of film loss by reaction with residual oxygen, but our equipment setup did not allow us to carry out such an experiment.

Thermal Characterization of GO. We performed thermogravimetric and differential scanning calorimetric analysis of our dry GO powder, running under purified nitrogen gas flow with a 5 °C/min heating rate.

XPS Analysis of Reduced GO. We probed the nitrogen content of our GO films by taking narrow scans of the C 1s and N 1s region using XPS, PHI-5000 Versaprobe (ULVAC-PHI Inc., Osaka, Japan). Spectra were baseline corrected and energy shifted using the instrument software.

Acknowledgment. We thank Colin C. Reese for access to and training in the use of the glass-tube furnace with controlled argon flow. Z. Bao acknowledges financial support from the Center for Polymeric Interfaces and Macromolecular Assemblies (NSF-Center MRSEC under Award Number DMR-0213618), from a 3M Faculty Award and from a Sloan Research Fellowship. Y. Chen gratefully acknowledges the financial support from MoST (#2006CB0N0702), MoE (#20040055020), and the NSF (#20774047 and 60676051) of China.

Supporting Information Available: Size distribution of graphene nanosheets, details of film thickness measurements with AFM, and correlation of solution concentration vs film thickness for single-spinned substrates. This information is available free of charge *via* the Internet at http://pubs.acs.org.

REFERENCES AND NOTES

1. Hummers, Wm. S., Jr.; Offeman, R. E. Preparation of Graphitic Oxide. *J. Am. Chem. Soc.* **1958**, *80*, 1339.
2. Schniepp, H. C.; Li, J.; McAllister, M. J.; Sai, H.; Herrera-Alonso, M.; Adamson, D. H.; Prud'homme, R. K.; Car, R.; Saville, D. A.; Aksay, I. A. Functionalized Single Graphene Sheets Derived from Splitting Graphite Oxide. *J. Phys. Chem. B* **2006**, *110*, 8535–8539.
3. Stankovich, S.; Dikin, D. A.; Piner, R. D.; Kohlhaas, K. A.; Kleinhammes, A.; Jia, Y.; Wu, Y.; Nguyen, S. T.; Ruoff, R. S. Synthesis of Graphene-Based Nanosheets via Chemical Reduction of Exfoliated Graphite Oxide. *Carbon* **2007**, *45*, 1558–1565.
4. McAllister, M. J.; Li, J.; Adamson, D. H.; Schniepp, H. C.; Abdala, A. A.; Liu, J.; Herrera-Alonso, M.; Milius, D. L.; Car, R.; Prud'homme, R. K.; Aksay, I. A. Single Sheet Functionalized Graphene by Oxidation and Thermal Expansion of Graphite. *Chem. Mater.* **2007**, *19*, 4396–4404.
5. Szabo, T.; Berkesi, O.; Forgo, P.; Josepovits, K.; Sanakis, Y.; Petridis, D.; Dekany, I. Evolution of Surface Functional Groups in a Series of Progressively Oxidized Graphite Oxides. *Chem. Mater.* **2006**, *18*, 2740–2749.
6. Stankovich, S.; Piner, R. D.; Chen, X.; Wu, N.; Nguyen, S. T.; Ruoff, R. S. Stable Aqueous Dispersions of Graphitic Nanoplatelets via the Reduction of Exfoliated Graphite Oxide in the Presence of Poly(sodium 4-styrenesulfonate). *J. Mater. Chem.* **2006**, *16*, 155–158.
7. Dikin, D. A.; Stankovich, S.; Zimney, E. J.; Piner, R. D.; Dommett, G. H. B.; Evmenenko, G.; Nguyen, S. T.; Ruoff, R. Preparation and Characterization of Graphene Oxide Paper. *Nature* **2007**, *448*, 457–460.
8. Stankovich, S.; Dikin, D. A.; Dommett, G. H. B.; Kohlhaas, K. M.; Zimney, E. J.; Stach, E. A.; Piner, R. D.; Nguyen, S. T.; Ruoff, R. S. Graphene-Based Composite Materials. *Nature* **2006**, *442*, 282–286.
9. Ramanathan, T.; Stankovich, S.; Dikin, D. A.; Liu, H.; Shen, H.; Nguyen, S. T.; Brinson, L. C. Graphitic Nanofillers in PMMA Nanocomposites-An Investigation of Particle Size and Dispersion and their Influence on Nanocomposite Properties. *J. Polym. Sci., Part B: Polym. Phys.* **2007**, *45*, 2097–2112.
10. Watcharotone, S.; Dikin, D. A.; Stankovich, S.; Piner, R.; Jung, I.; Dommett, G. H. B.; Evmenenko, G.; Wu, S.; Chen, S.; Liu, C.; Nguyen, S. T.; Ruoff, R. S. Graphene-Silica Composite Thin Films as Transparent Conductors. *Nano Lett.* **2007**, *7*, 1888–1892.
11. Novoselov, K. S.; Geim, A. K.; Morozov, S. V.; Jiang, D.; Zhang, Y.; Dubonos, S. V.; Grigorieva, I. V.; Firsov, A. A. Electric Field Effect in Atomically Thin Carbon Films. *Science* **2004**, *306*, 666–669.
12. Gilje, S.; Han, S.; Wang, M.; Wang, K. L.; Kaner, R. B. A Chemical Route to Graphene for Device Applications. *Nano Lett.* **2007**, *7*, 3394–3398.
13. Wu, S.; Yang, D. *Fundamentals of Liquid Crystal Devices*; Wiley: Wiltshire, U.K., 2006.
14. Betz, U.; Kharrazi, O.,M.; Marthy, J.; Escola, M. F.; Atamny, F. Thin Films Engineering of Indium Tin Oxide: Large Area Flat Panel Displays Application. *Surf. Coat. Technol.* **2006**, *200*, 5751–5759.
15. Kim, U. J.; Liu, X. M.; Furtado, C. A.; Chen, G.; Saito, R.; Jiang, J.; Dresselhaus, M. S.; Eklund, P. C. Infrared-Active Vibrational Modes of Single-Walled Carbon Nanotubes. *Phys. Rev. Lett.* **2005**, *95*, 157402/1–157402/4.
16. Donner, S.; Li, H. W.; Yeung, E. S.; Porter, M. D. Fabrication of Optically Transparent Carbon Electrodes by the Pyrolysis of Photoresist Films: Approach to Single-Molecule Spectroelectrochemistry. *Anal. Chem.* **2006**, *78*, 2816–2822.
17. Hirata, M.; Gotou, T.; Horiuchi, S.; Fujiwara, M.; Ohba, M. Thin-Film Particles of Graphite Oxide 1: High-Yield Synthesis and Flexibility of the Particles. *Carbon* **2004**, *42*, 2929–2937.

18. Gomez-Navarro, C.; Weitz, R. T.; Bittner, A. M.; Scolari, M.; Mews, A.; Burghard, M.; Kern, K. Electronic Transport Properties of Individual Chemically Reduced Graphene Oxide Sheets. *Nano Lett.* **2007**, *7*, 3499–3503.
19. Lerf, A.; He, H.; Forster, M.; Klinowski, J. Structure of Graphite Oxide Revisited. *J. Phys. Chem. B* **1998**, *102*, 4477–4482.
20. Forbeaux, I.; Themlin, J. M.; Debever, J. M. Heteroepitaxial Graphite on 6H-SiC (0001): Interface Formation through Conduction-Band Electronic Structure. *Phys. Rev. B* **1998**, *58*, 16396.
21. Berger, C.; Song, Z.; Li, X.; Wu, X.; Brown, N.; Naud, C.; Mayou, D.; Li, T.; Hass, J.; Marchenkov, A. N.; Conrad, E. H.; First, P. N.; de Heer, W. A. Electronic Confinement and Coherence in Patterned Epitaxial Graphene. *Science* **2006**, *312*, 1191–1196.
22. Wang, X; Zhi, L.; Müllen, K. Transparent, Conductive Graphene Electrodes for Dye-Sensitized Solar Cells. *Nano Lett.* **2007**, *8*, 323–327.
23. Contreras, M. A.; Barnes, T.; van de Lagemaat, J.; Rumbles, G.; Coutts, T. J.; Weeks, C.; Glatkowski, P.; Levitsky, I.; Peltola, J.; Britz, D. A. Replacement of Transparent Conductive Oxides by Single-Wall Carbon Nanotubes in Cu(In,Ga)Se2-Based Solar Cells. *J. Phys. Chem. C* **2007**, *111*, 14045–14048.
24. Wu, Z. C.; Chen, Z. H.; Du, X.; Logan, J. M.; Sippel, J.; Nikolou, M.; Kamaras, K.; Reynolds, J. R.; Tanner, D. B.; Hebard, A. F.; Rinzler, A. G. Transparent, Conductive Carbon Nanotube Films. *Science* **2004**, *305*, 1273–1276.
25. Rowell, M. W.; Topinka, M. A.; McGehee, M. D.; Prall, H.; Dennler, G.; Sariciftci, N. S.; Hu, L.; Gruner, G. Organic Solar Cells with Carbon Nanotube Network Electrodes. *Appl. Phys. Lett.* **2006**, *88*, 233506/1–233506/3.
26. Gruner, G. Carbon Nanotube Films for Transparent and Plastic Electronics. *J. Mater. Chem.* **2006**, *16*, 3533–3539.
27. Hu, L.; Gruner, G.; Gong, J.; Kim, C.; Hornbostel, B. Electrowetting Devices with Transparent Single-Walled Carbon Nanotube Electrodes. *Appl. Phys. Lett.* **2007**, *90*, 093124/1–093124/3.
28. Stotter, J.; Show, Y.; Wang, S. H. Swain, Comparison of the Electrical, Optical, and Electrochemical Properties of Diamond and Indium Tin Oxide Thin-Film Electrodes. *Chem. Mater.* **2005**, *17*, 4880–4888.
29. Stankovich, S.; Piner, R. D.; Nguyen, S. T.; Ruoff, R. S. Synthesis and Exfoliation of Isocyanate-Treated Graphene Oxide Nanoplatelets. *Carbon* **2006**, *44*, 3342–3347.
30. Niyogi, S.; Bekyarova, E.; Itkis, M. E.; McWilliams, J. L.; Hamon, M. A.; Haddon, R. C. Solution Properties of Graphite and Graphene. *J. Am. Chem. Soc.* **2006**, *128*, 7720–7721.
31. Worsley, K. A.; Ramesh, P.; Mandal, S. K.; Niyogi, S.; Itkis, M. E.; Haddon, R. C. Soluble Graphene Derived from Graphite Fluoride. *Chem. Phys. Lett.* **2007**, *445*, 51–56.
32. Lee, S. T.; Gao, Z. Q.; Hung, L. S. Metal Diffusion From Electrodes in Organic Light-Emitting Diodes. *Appl. Phys. Lett.* **1999**, *75*, 1404–1406.